Evaluation of Myocardial Infarct Size Before and After Reperfusion: Dual-Tracer Imaging with Radiolabeled Antimyosin Antibody

Jagat Narula, Philip D. Nicol, James F. Southern, Pierluigi Pieri, Sean M. O'Donnell, J. Luis Guererro, Naseem D. Nossiff, John B. Newell, H. William Strauss and Ban-An Khaw

Cardiac Unit, Division of Nuclear Medicine and Department of Pathology, Massachusetts General Hospital and Harvard Medical School; and Center for Drug Targeting and Analysis, Northeastern University, Boston, Massachusetts

Antimyosin antibody is a specific marker of myocardial necrosis that is based on the loss of integrity of the sarcolemmal membrane. Because antimyosin can be labeled with several different radiotracers, gamma imaging performed with antimyosin labeled with two different radionuclides can be used to quantify infarct size before and after an intervention such as reperfusion. **Methods:** Twelve open-chested anesthetized dogs were evaluated both at the end of 1.5 hr of occlusion of the left anterior descending coronary artery and following reperfusion. Antimyosin Fab radiolabeled with either ^{123}I or ^{111}In was injected by intracoronary administration over 3 min at the end of the occlusion interval, and the coronary sinus was drained continuously for 7 min to prevent recirculation of the antibody. One hour after reperfusion, a second injection of antimyosin Fab (labeled with a different isotope from the first) was administered as before. Six dogs were given intracoronary trifluoperazine (150 μg/kg of body weight) simultaneously with reperfusion, and another six dogs received saline as the control. The infarct size in grams before and after reperfusion was assessed by antimyosin antibody uptake in ex vivo images of 1-cm thick slices of the hearts. The mean infarct sizes before (W1) and after (W2) reperfusion were then calculated as the percent of infarcted myocardium/ventricular myocardial mass. **Results:** There was a significant increase in the mean percent infarct size after reperfusion in the control group (W2 = 16.73 ± 4.0, W1 = 14.92 ± 3.88; p = 0.029). The mean infarct size was uniformly smaller with trifluoperazine intervention (W2 = 12.33 ± 2.03, W1 = 16.34 ± 2.78; p = 0.004). The difference between the mean change in the infarct sizes in the two groups was highly significant (p = 0.002). **Conclusion:** Dual imaging of the extent of myocardial necrosis before and after an intervention (reperfusion) in the same animal demonstrated the utility of antimyosin imaging to document changes in the extent of necrosis.

Key Words: myocardial infarct size; antimyosin antibody; myocardial reperfusion

J Nucl Med 1994; 35:1076–1085

The restoration of blood flow to ischemic myocardium reduces the loss of functional tissue and exerts beneficial effects in addition to the actual mass of myocardium salvaged by the prevention of infarct expansion, ventricular dilatation, formation of aneurysm and heart failure (*1*). Reperfusion also demonstrates deleterious effects, with accelerated tissue damage caused by the production of oxygen-derived free radicals and calcium paradox, resulting in prolonged postischemic depression of ventricular functions and the no-reflow phenomenon (*1–5*). Most experimental models of reperfusion injury and therapeutic interventions use only a single assessment of infarct size within a given animal (*6–11*). Because the development of necrosis is a process that requires time, the selection of the interval between reperfusion and the measurement of its effects can alter the results. It would be helpful to measure the extent of necrosis at several time points, both before and after reperfusion or an intervention in the same animal. The occurrence of reperfusion injury was recently reported by a pathologic comparison of horseradish peroxidase and triphenyl tetrazolium chloride delineated pre- and postreperfusion infarct sizes in the same animal (*12*).

Antimyosin antibody reliably identifies the extent of myocardial necrosis (*13–15*). Because the antibody can be labeled with several radionuclides, it is possible to define the extent of necrosis with this marker at two different (or more) times. This technique would permit each animal to serve as its own control. To test the validity of dual imaging of an infarcted zone by antimyosin antibody, the present study was performed to determine the effect of a major intervention and reperfusion on the immediate extent of necrosis. In addition, a second group of animals treated with trifluoperazine (TFP), a member of the phenothiazine family, were studied to determine whether this drug could limit the initial damage to the sarcolemma. Pretreatment with phenothiazines was reported to limit the extent of myocyte necrosis by preventing degradation of the membrane phospholipids and restricting calmodulin-dependent calcium influx (*16–22*). Of the phenothiazines, TFP is known to have the maximum relative calmodulin-binding activity (*23,24*).

Received Sept. 27, 1993; revision accepted Mar. 9, 1994.

For correspondence or reprints contact: Ban An Khaw, PhD, Center for Drug Targeting and Analysis, Mugar-205, Bouvé College of Pharmacy and Health Sciences, Northeastern University, Boston, MA 02115.

MATERIAL AND METHODS

Antimyosin Antibodies and Radiolabeling

A monoclonal antimyosin antibody (R11D10, Centocor, Malvern, PA) was generated by hybridization of immune murine spleen cells with SP2/OA murine myeloma cells and purified by the methods previously described (*25*). The bicyclic anhydride of diethylenetriamine pentaacetic acid (DTPA) was prepared by the method of Hnatowich et al. (*26*) for coupling with antimyosin-Fab. The molar ratio of DTPA to Fab was 1:1. Two approaches were used to label DTPA-antimyosin Fab, ^{111}In was coupled to the DTPA and ^{123}I was coupled directly to the protein using chloramine-T.

Indium Labeling. Approximately 37 MBq (1 mCi) of ^{111}InCl was used to label 100 μg of DTPA-R11D10-Fab. To a 1-mCi aliquot (50 μl) of ^{111}InCl, an equal volume of 1 *M* sodium citrate (pH 5.5) was added, followed by an aliquot of antimyosin-Fab. The reaction mixture was allowed to incubate at room temperature for 30 min. Antibody-bound ^{111}In was separated from free ^{111}In by Sephadex (Sigma Chemical, St. Louis, MO) G-25 column (10 ml) chromatography. The peak tubes in the void volume containing the radiolabeled antibody were pooled and used within 1 hr of radiolabeling. An average of 80% of the initial antibody concentration was recovered in the peak tubes containing the radiolabeled antibody.

Iodination. Radioiodination was accomplished by the chloramine-T method, as described by Hunter and Greenwood (*27*) to label R11D10 Fab with ^{123}I. To a 100-μg aliquot of DTPA-coupled R11D10 Fab antimyosin antibody in 0.1 *M* phosphate buffer (pH 7.4), 37 MBq (1 mCi) of ^{123}I was added and mixed thoroughly. A 10-μl aliquot of chloramine-T (26 mg/ml in 0.5 *M* phosphate buffer, pH 7.4) was added followed by mixing for 2 min. Iodination was terminated by the addition of 25 μl of 0.1 *M* methionine plus 0.1 *M* cresol. The reaction mixture was then applied to a 10-ml Sephadex G-25 column to separate free and protein-bound radioiodine, as described earlier.

Experimental Protocol

Twenty mongrel dogs of both sexes weighing 20 to 30 kg were anesthetized with intravenous sodium pentobarbital (30 mg/kg) and ventilated with a Harvard positive-pressure respirator (Harvard Apparatus, South Natick, MA) The right femoral artery and vein were isolated and catheterized to facilitate monitoring of arterial pressures and the administration of medication. Arterial pressure and a multilead electrocardiogram were continuously monitored. A left thoracotomy was performed, and the heart was suspended in the pericardial cradle. Proximal and midportions of left anterior descending coronary artery (LAD) were isolated, and a surgical monofilament snare enclosed in polyethylene tubing was placed immediately distal to the first diagonal branch. A small branch just distal to the site of occlusion was cannulated with a 22-gauge catheter for the administration of antimyosin into the postocclusion segment of the LAD. Following the administration of 4000 units of heparin, two small incisions were made in the right atrium, and two limbs of a Y-shaped shunt were placed into the right atrial cavity, one of which was advanced into the coronary sinus. The coronary sinus cannula was secured by a suture placed exteriorly from the posterior aspect of the heart. The sinoatrial shunt provided the means for draining the coronary venous flow or allowing normal drainage of coronary venous blood into the right atrium (Fig. 1). A small incision was also made in the left atrial appendage for placement of a left atrial line.

The LAD was occluded by tightening the snare, and a prophylactic lidocaine infusion of 0.1 mg/kg was maintained for 1 hr. Three animals died as a result of ventricular fibrillation during the first 10 to 30 min of the LAD occlusion. At 1.5 hr of the LAD occlusion, the first assessment of the infarct size was made in the remaining 17 dogs (Fig. 2). The LAD territory was then reperfused by the removal of the snare. At the time of reperfusion, eight animals were randomly selected to receive a single 150-μg/kg dose of TFP (Sigma, St. Louis, MO) dissolved in 10 ml of 0.9 percent saline through the LAD cannula at a rate of 1.1 ml/min. The remaining nine animals received the same volume of intracoronary saline. After 1 hr of reperfusion, a second assessment of the infarct size was made (Fig. 2). Before killing the animals, 6 ml of monastral blue was injected through the coronary artery cannula distal to the occlusion for delineation of the area at risk by the identical protocol to antibody administration (described later). The animals were then killed by atrial injection of 20 to 40 mEq of potassium chloride. The heart was excised, the atria were removed, and the ventricular mass was recorded in grams.

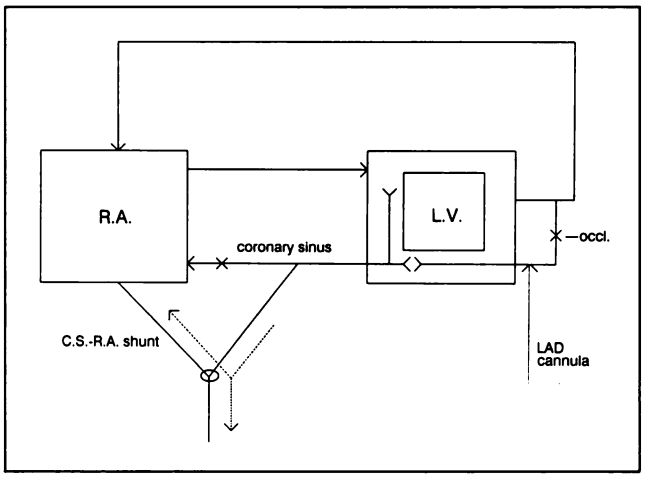

FIGURE 1. A Y-shaped shunt was placed into the right atrial cavity with one arm advanced into the coronary sinus and ligated in place. The shunt allowed normal coronary sinus flow into the right atrium and selective drainage of coronary venous blood during antibody injection.

Radiolabeled Antimyosin Antibody Injections. Radiolabeled antimyosin antibodies were administered through the LAD cannula with the snare in the occluded position. Approximately 40 to 60 μg of antimyosin Fab with 15 to 22.5 MBq (400–600 μCi) of radiolabel in 30 ml of lactated Ringer's was injected at the rate of 10 ml/min for 3 min. The coronary sinus was continuously drained during the injection and for an additional 4 min to prevent systemic circulation of the antibody. The coronary sinus effluent was collected in 1-min fractions. From every 1-min fraction, 100-μl aliquots of the coronary venous samples were counted to evaluate the recovery of the total injected dose. Corresponding 1-ml blood samples from the femoral artery were also withdrawn to assess whether there had been a spillage of antimyosin antibody into the systemic circulation. The coronary venous and femoral arterial samples were counted in a LKB 1282 Compugamma well scintillation counter (Pharmacia LKB Nuclear, Inc., Caithersburg, MD adjusted to record the photopeaks of ^{111}In and ^{123}I, using automatic background and spill corrections.

Antimyosin Antibody Imaging. The following sets of images were recorded in each animal: in vivo during the experiment, of the whole heart ex vivo and as 1-cm ring slices cut perpendicular

to the long axis of the left ventricle. Scintigraphic images were obtained using a gamma camera (Ohio-Nuclear 100, Solon, OH) equipped with a medium-energy collimator. The pulse height analyzer were set at center lines of 247 and 159 keV with 20% windows for ^{111}In and ^{123}I radioisotopes, respectively. Concurrent with antibody injections, sequential 1-min acquisition images were recorded for a total of 8 min. The excised hearts were imaged whole and as 1-cm thick slices for both isotopes. Background images were also collected at each isotope setting for identical acquisition time. The background corrected and peak-normalized sets of images were recorded on floppy disks and the experiment number, treatment and sequence of injection of ^{111}In- and ^{123}I-labeled antimyosin antibody were blinded. The infarct size was assessed twice individually by three observers. Semiautomatic planimetry was performed with a Technicare 560 computer (Technicare Corp., Solon, OH) to determine the infarct size as the number of pixels, as previously described (*28*). The pixel size was calibrated, and the absolute volume of infarcted tissue was determined (area × slice thickness). This value, multiplied by the specific gravity of myocardium (1.05), was used to determine the weight of the infarcted tissue in grams (*29*). The percent infarct relative to the ventricular mass was then calculated for the statistical analysis.

Standardization of the Model

To ensure the accuracy and reproducibility of the model, pilot studies were performed to standardize the intracoronary injection of antimyosin in animals with experimental myocardial infarction. In six animals, the rate of radiolabeled antibody administration was determined that would adequately and reproducibly perfuse the area under observation and not result in a streaming effect. The distribution appeared to be uniform at an injection rate of 10 ml/min, approximately the rate of the coronary blood flow. The injections were performed in both the opened and occluded artery. It was observed that injections during occlusion provided more reproducible delivery into the zone at risk.

In two different animals, two sets of antimyosin antibody radiolabeled with different isotopes were injected simultaneously after a similar 2.5 hr of ischemia followed by reperfusion to identify whether the order of ^{111}In- or ^{123}I-labeled antibody injection resulted in a difference in the infarct sizes. No differences in the infarct sizes were observed in this study in which antimyosin antibody radiolabeled with these two different radioisotopes was administered simultaneously. Quantitatively, the infarct sizes determined by ^{123}I antimyosin were within ±0.42 g (±0.25% of the left ventricular mass) from those by ^{111}In antimyosin.

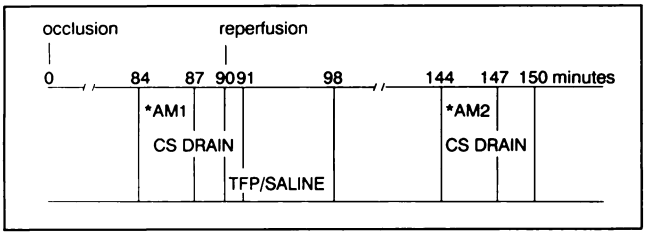

FIGURE 2. LAD was occluded for 1.5 hr followed by reperfusion for 1 hr. Six minutes prior to reperfusion either ^{111}In- or ^{123}I-labeled antimyosin Fab (AM1) was injected into the LAD distal to the occlusion. Antimyosin antibody (100 μg) with 15 to 22.5 MBq of radiolabel in 30 ml of lactated Ringer's was injected at the rate of 10 ml/min for 3 min. The coronary sinus (CS) was continuously drained during the injection and for additional 3 to 4 min to obviate systemic recirculation of antibodies. This allowed the first-pass delineation of the pre-reperfusion infarct size. Simultaneously with the reperfusion, 10 ml of 0.9 percent saline with or without 150 μg/kg of TFP was infused through the LAD cannula over a period of 8 min. After 1 hr of reperfusion, the postreperfusion infarct size was demarcated by antimyosin antibody radiolabeled with the isotope that was not used for the first injection (AM2).

Because the lower peak energy of emission of ^{111}In (173 keV) is close to that of ^{123}I (159 keV), there was a potential for cross-talk. The cross-talk between these two isotope window settings was found to be 9%. However, to minimize any potential effects of cross-talk, the sequence of radioisotope administration was alternated with each successive animal study. This process should neutralize the sole effect of cross-talk. In the present study, both placebo- and TFP-treated groups had ^{123}I antimyosin as the first injection in one half of the number of animals and ^{111}In antimyosin as the first injection in the remaining half of the group.

To enable quantitation of the differences in the infarct size at two time periods, the inadvertent entry of the first radiolabeled antibody into the systemic circulation must be absolutely avoided. In the preliminary studies, the coronary sinus drainage was performed up to 12 min after antimyosin antibody injection, and the proportion of the recovery of the total injected dose of the radioactivity was assessed at every minute, as described. Because all activity was recovered within 5 min, the protocol for the study used 7 min to ensure capture of all activity appearing in the coronary sinus. To ensure that no radiolabeled antimyosin entered the systemic circulation, arterial blood was sampled from the femoral artery.

In the present study, a continuous antibody infusion into the infarct zone was administered through the coronary artery over a period of 3 min. Theoretically, this appears to be a substantially long perfusion time for a high-affinity antibody like R11D10 (K_a = $0.5–1.0 \times 10^{-9}$ l/*M*). However, to determine whether a single pass of antimyosin antibody over the infarct was adequate, the percent of the injected dose per gram sequestered in the infarcted myocardium was evaluated. The data available from the standardization experiments demonstrated that the mean percent dose per gram was 0.1312 (95% confidence interval, 0.0644–0.198; maximum, 0.2266%) for ^{123}I and 0.1322 (95% confidence intervals, 0.0236–0.2408; maximum, 1.42%) for ^{111}In-labeled antimyosin antibody. These data are comparable to the uptake of radioactivity in the infarcted myocardium after the intravenous injection of radiolabeled antimyosin antibody with 4 hr of recirculation (mean percent injected dose per gram, 0.1335; standard deviation, 0.0187) (*30*). The lack of activity in the noninvolved coronary territory as a result of coronary sinus diversion in the present study offered a better target-to-nontarget contrast for imaging compared with the standard recirculation experiments.

To test for a possible interaction between antimyosin and TFP that could inhibit the binding of the antibody to myosin, serial dilutions of antimyosin R11D10 Fab (range 0.1–100 μg/ml) were tested for binding to human left ventricular cardiac myosin in the presence of varying concentrations (2.5, 25 and 250 μg/ml) of TFP. A negative-control antidigoxin antibody was also included in the test. An ^{125}I-labeled goat anti-mouse Fab antibody was used as a second antibody to evaluate the relative degree of binding. TFP did not show any inhibitory effect on the binding of antimyosin Fab to the homologous antigen (Fig. 3).

Five animals were excluded from the analysis before calculation of the infarct size. In two animals, there was high systemic activity of antimyosin Fab; in two other cases, the first and second antibody deliveries were dissimilar (resulting from streaming ef-

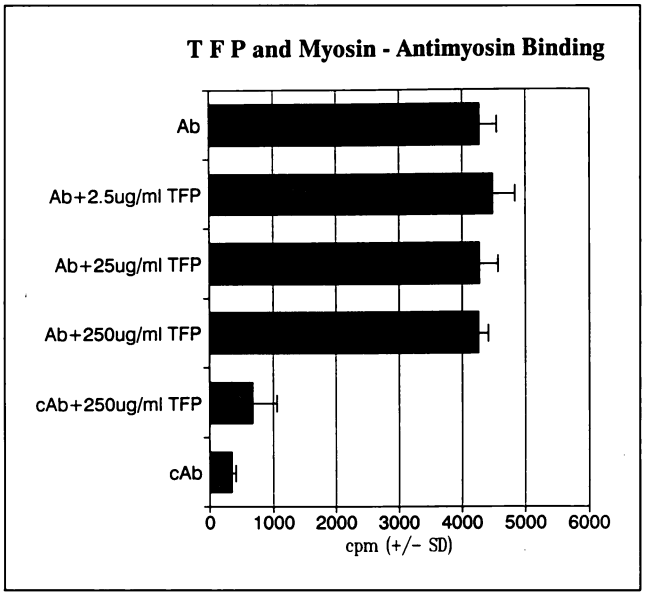

FIGURE 3. Binding of serial dilution of antimyosin antibody (Ab; range 0.1–100 μg/ml) to left ventricular human heart myosin in the presence of varying concentrations (2.5, 25 and 250 μg/ml) of TFP. Antidigoxin antibody was used as a negative control (cAb). TFP did not interfere with the binding of antimyosin antibody.

fect). In the fifth case, no imaging could be performed with one isotope, which again could represent dissimilar delivery. The use of these exclusion criteria incidentally left equal numbers of animals (n = 6 + 6) in the control and treated groups.

Statistical Analyses

Data representing the antimyosin-delineated infarct sizes (assessed in grams and the percent infarct relative to the ventricular mass) were analyzed in a three-way factorial analysis of variance (ANOVA) with the use of the BMDP program P4V (University of California, Berkeley, CA) (*31*). One grouping (or "between") factor had two levels, control dogs and dogs treated with TFP. Two trial (or "within") factors were included in the ANOVA design. One trial factor was the time of measurement with the two levels: prereperfusion and postreperfusion. Another trial factor was the observer(s). The infarct size, measured twice by three independent observers, and the measurements resulting from these three observers, were treated as three different levels of the trial factor (for the analysis of intra- and interobserver differences). For final infarct size calculations, the mean infarct size was obtained from the six observations. Only one of the 72 observations made by the three observers was discordant. All possible interactions among the three factors; grouping, time of measurement and observer, were assessed and multiple-comparison protection was provided by the Bonferroni method (main effects and interactions give seven effects, which require a threshold for significance of alpha = 0.05/7 = .007) (*32*). The null hypothesis, that treatment with TFP at reperfusion would result in the same increment in infarct size (from prereperfusion to postreperfusion) as would treatment with saline, was regarded as disproved by the significant time of measurement × grouping interaction.

Histopathologic Examination

Histopathologic studies were performed in four control and two test animals chosen at random. Full-thickness slice sections were obtained from the center of the infarct and from the periphery of the infarct, as determined by the monastral blue-stained areas. Tissue sections were also obtained from the distal uninvolved myocardium for comparative examination. The tissue sections were fixed in formaldehyde, dehydrated and embedded in paraffin. The sections were cut and stained with hematoxylin and eosin and examined by light microscopy in a blinded manner for the presence of contraction bands, myocyte necrosis and the degree of neutrophil infiltration. Representative specimens from both the control and TFP-treated animals from the central infarct zone, the peripheral infarct zone and distal uninvolved myocardium were also examined ultrastructurally for evidence of reversible or irreversible ischemic injury. Immediately following death, 1-mm^3 specimens from the designated myocardial regions were placed in glutaraldehyde and then processed in Epon (EM Science, Ft. Washington, PA) by standard techniques. Thin 0.1-μ sections were examined using a Phillips 100 electron microscope (N.V. Phillips, Eindhoven, Holland).

RESULTS

The similarity of delivery of the two radiotracers was confirmed by three observers independently for each study from sequential acquisition images of the first (Fig. 4, top) and second radiolabeled antibody delivery (bottom). Approximately 60%–70% of the total injected dose was recovered from the coronary venous blood. Negligible activity was observed in the systemic circulation (Fig. 5), confirming the effective drainage of the antibody.

The initial mean infarct size determined as the percent infarct relative to ventricular mass at 1.5 hr after coronary occlusion (W1) was 14.92 ± 3.88% (or 24.18 ± 6.28 g) (mean ± s.e.m.) in the control group and 16.34 ± 2.78% (or 28.13 ± 4.05 g) in the treated group (Table 1). There was no statistically significant difference between the mean prereperfusion infarct sizes of the two groups (p = 0.77). After

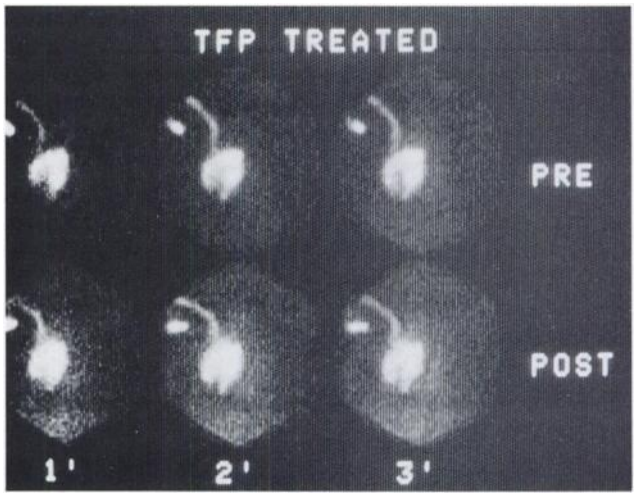

FIGURE 4. Antimyosin antibody infusion at 10 ml/min into the occluded LAD reproducibly perfused the zones at risk, as shown by sequential 1-min acquisition images recorded during antibody infusion. The top panels show prereperfusion antimyosin antibody delivery, and the bottom panels show 1-hr postreperfusion antimyosin antibody delivery. The sequential images document similar delivery of the antibody on the two occasions.

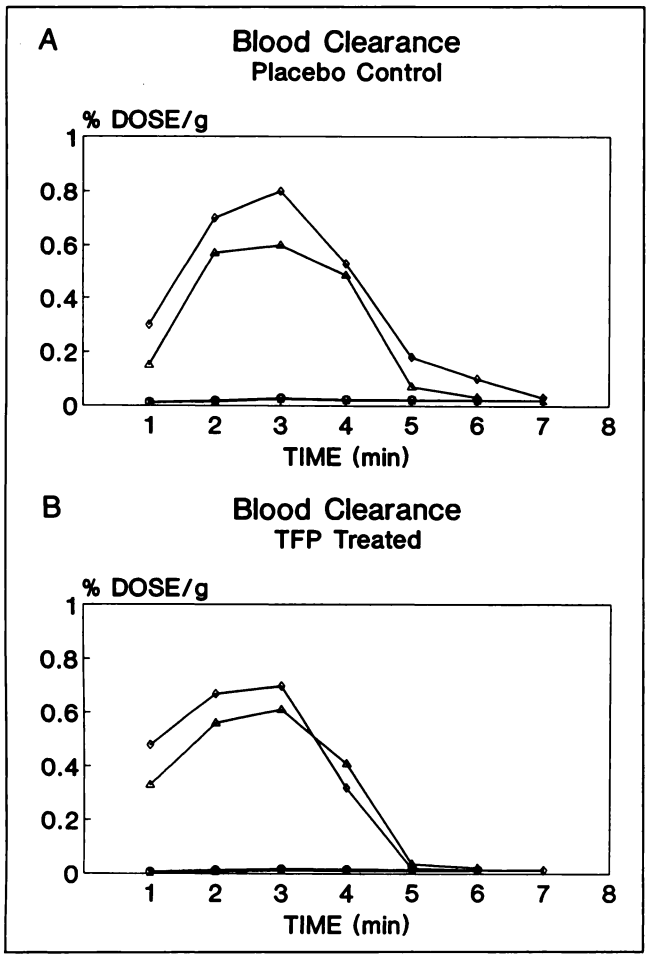

FIGURE 5. Blood activities in the coronary sinus effluent during the first (◇) and second (△) antibody injections compared with the corresponding femoral artery blood samples (×, ○) in placebo control (A) and TFP-treated (B) animals. No radioactivity was found in the systemic circulation, confirming the effectiveness of coronary sinus drainage and single-pass antimyosin antibody binding to the infarcted zones.

reperfusion, there was a significant increase in the infarct size (W2 = 16.73 ± 4.0% of ventricular mass or 28.02 ± 6.38 g) in the control group (p = 0.029). Five of the six control animals demonstrated a greater postreperfusion infarct size (Fig. 6A and B, arrows), and one control animal showed a decrease in the infarct size (Fig. 7A). In the TFP-treated group, there was a visible decrease in the postreperfusion infarct sizes in the images of the heart slices (Fig. 6C and D, arrows). A uniform decrease in the overall infarct size was observed (W2 = 12.33 ± 2.03% ventricular myocardial mass or 21.25 ± 2.93 g; p = 0.004; Fig. 7B).

TABLE 1
Pre- and Postreperfusion Percent Infarct Sizes Relative to Ventricular Myocardial Mass (mean ± s.e.m.)

Infarct size	Control (%)	TFP (%)	p value
Prereperfusion (W1)	14.92 ± 3.88	16.34 ± 2.78	0.77
Postreperfusion (W2)	16.73 ± 4.00	12.33 ± 2.03	0.35
Postprereperfusion (W2 − W1)	1.80 ± 1.19	−4.0 ± 1.82	0.002
p value	0.029	0.004	

TFP = trifluoperazine.

None of the statistical main effects (time of measurement, observers and grouping) and the interactions (except the time of measurement × grouping) was significantly different. The time of measurement by grouping interaction was significantly different from zero (p = 0.002), indicating that the mean change in infarct size (12% increase in prereperfusion infarct size = 3.83 ± 2.26 g) after reperfusion in the control group was significantly greater than the mean change in infarct size after reperfusion in the TFP-treated group (24.5% decrease in prereperfusion infarct size = −6.88 ± 1.26 g) (Fig. 7C).

The central infarct zone contained foci of myocyte necrosis and contraction bands. In the peripheral infarct, all four of four placebo control animals included in the histologic studies showed myocyte necrosis, as evidenced by contraction bands similar to but quantitatively less than those seen in the infarct center (Fig. 8A). By contrast, the periphery of infarct from animals treated with TFP (two of two for histologic examination) showed no light microscopic changes indicative of myocardial injury (Fig. 8B). The presence of monastral blue in both the control and treated myocardial samples from the peripheral infarct zone confirmed that both were from the zone at risk.

Ultrastructural examination of the infarct periphery showed that placebo treatment did not confer protection, as evidenced by the presence of amorphous densities or spicular aggregates, disruption of mitochondrial cristae, edema and I bands. These tissue samples also lacked glycogen granules (Fig. 9A). Sarcolemmal disruption was also evident in the electron micrographs of the placebo-treated heart sections (Fig. 9B). However, TFP treatment conferred myocardial protection, as evidenced by the presence of glycogen granules and lack of mitochondrial disruption and absence of I bands (Fig. 9C). Cellular swelling and edema were, however, present. In the center of the infarcts, placebo-treated myocardium showed extensive mitochondrial damage and lack of glycogen granules (Fig. 9D and E), but TFP-treated myocardium showed residual glycogen granules and restriction of myofibrillar relaxation (Fig. 9F). In normal, posterior left-ventricular myocardium from saline and TFP-treated animals, both demonstrated normal ultrastructure, including the presence of glycogen granules, intact sarcolemma and normal mitochondria (not shown).

DISCUSSION

Most experimental studies of reperfusion injury make only a single assessment of the infarct size in a given animal at a time point far removed from the reperfusion event

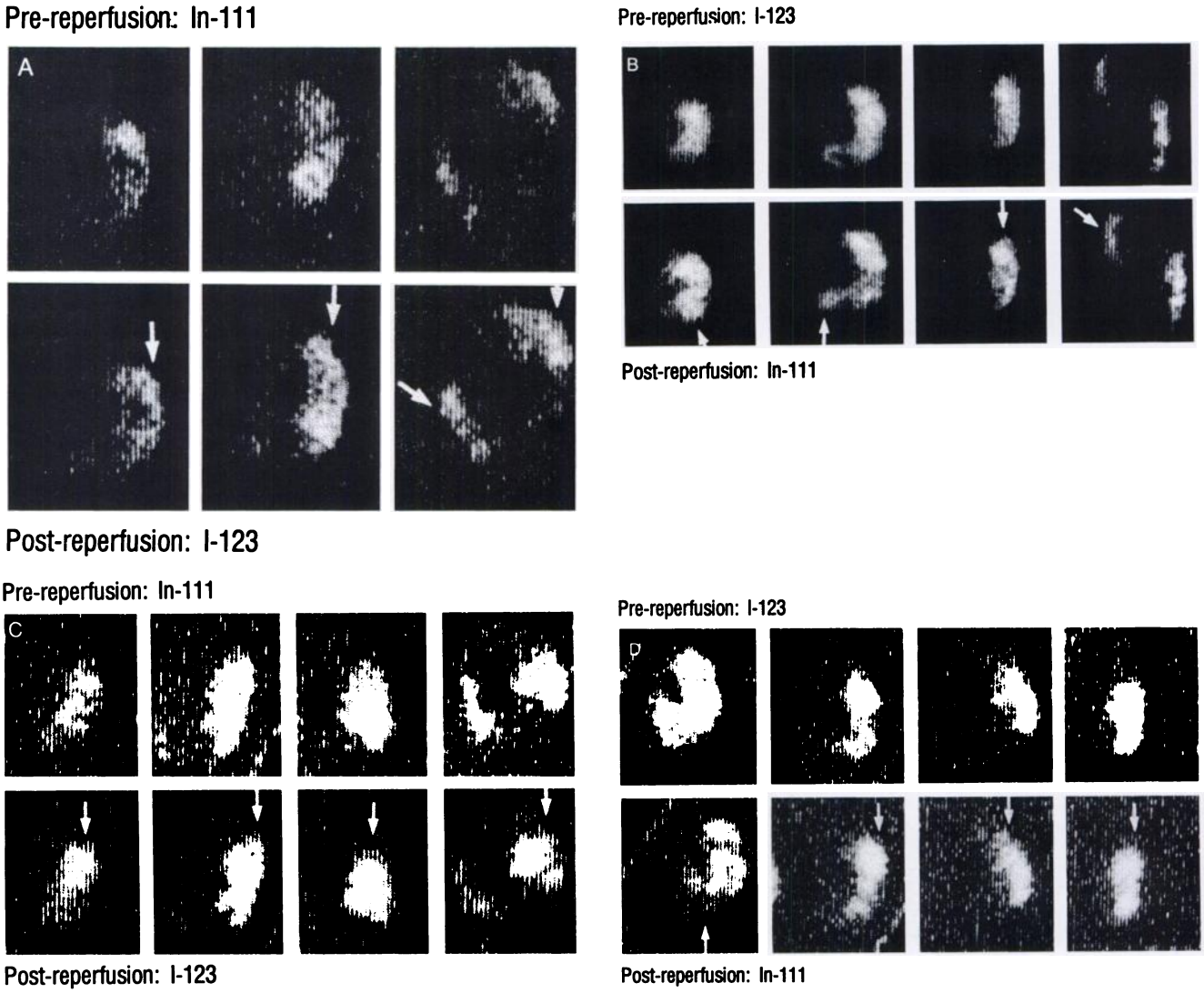

FIGURE 6. Peak-normalized gamma images of 1-cm thick slices of the hearts treated with saline (A and B) or TFP (C and D). A and C show ^{111}In-antimyosin Fab as the first administered radiolabeled antibody. B and D show the reverse sequence of radiolabeled antibody delivery with ^{123}I used as the first antibody injection. Prereperfusion images are shown in the top panel and postreperfusion images in the bottom panel. The postreperfusion images delineate larger areas of myocytic necrosis in control animals, irrespective of the radioisotope used (A and B, arrows). The infarct size is reduced in TFP-treated animals (C and D, arrows).

(*7–11*). The infarct size may vary considerably from animal to animal because of variations in the vascular supply, including collateralization. It has been recommended that the mass of the necrotic myocardium be plotted as a percentage of the zone at risk versus the subepicardial collateral blood flow within the zone at risk (*6*). Functional parameters, including angiographic left ventricular function (*11*) or sonometeric assessment of contractility indices (*10*) have also been used to evaluate the therapeutic effects of various agents in the prevention of reperfusion injury. Although these techniques correlate well with infarct size, they are not direct measures of infarct size. The present study provided an opportunity for the identification of infarct size before and after reperfusion in the same animal. The same indicator with two different radiolabels—antimyosin antibody—was used for dual imaging of the infarcts with single-pass binding of the antibody in the zone at risk. Because myocytes contain large concentrations of myosin and the amount of radiolabeled antimyosin antibody used is small, saturation of the antigenic sites, which could prevent binding of the second aliquot of the antibody, is not anticipated. The two crucial steps to ensure reproducibility and accuracy of the model were confirmation of the lack of systemic recirculation of antimyosin antibody and the similarity in delivery of the two tracers.

In the present study, five of the six control animals had significantly larger infarct sizes with reperfusion ($p = 0.029$). The increase in the infarct size may be a result of reperfusion injury or an inevitable consequence of previously ischemic myocytes. On the other hand, all six animals that received TFP demonstrated a decrease in infarct size of 24.5% of the prereperfusion infarct size by the scintigraphic technique ($p = 0.004$), and the histologic appearance suggested a true reduction in the extent of damage. A

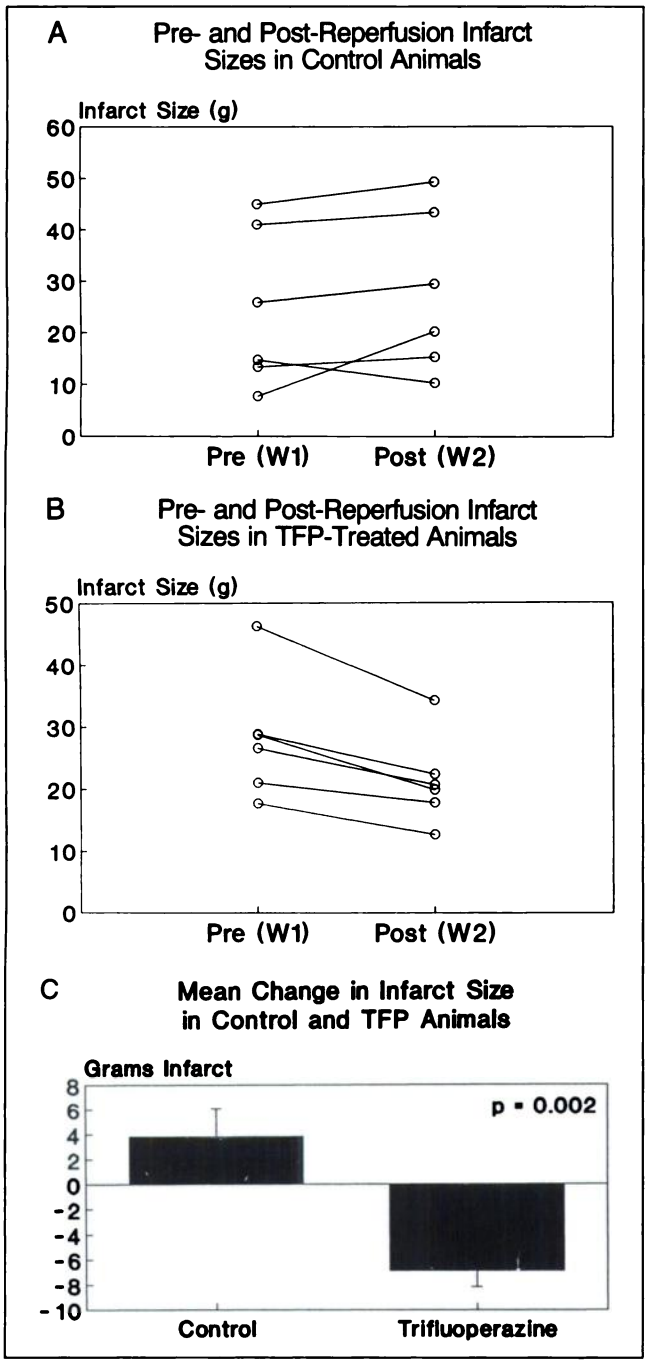

FIGURE 7. Infarct size (assessed in grams) was determined by the first and second radiolabeled antimyosin Fab in control (A) and TFP-treated (B) animals. Myocardial infarct size increased in five of the six control animals; it uniformly decreased in all TFP-treated experiments. Myocardial infarct size increased by 3.45 ± 2.03 g following reperfusion in control dogs but decreased by 6.88 ± 1.16 g in animals treated with TFP (C).

decrease in the infarct size may indicate some role for TFP in acutely reperfused infarcts. Phenothiazines prevent calcium fluxes across a variety of cell membranes (*33–36*) and are potent inhibitors of phospholipases, including some of lysosomal origin (*37–39*). The protective effect is probably associated with the reduced levels of cellular and mitochondrial calcium ions and stabilization or expansion of membranes.

Chlorpromazine pretreatment demonstrated a profound protective effect against ischemic rat liver cell death (*40*). There was little or no evidence of liver necrosis at 24 hr after reflow in chlorpromazine-pretreated animals that sustained up to 3 hr of ischemia. There was more than a twofold increase in the ability of the pretreated cells, compared with the untreated ischemic liver cells, to regenerate ATP. Furthermore, there was more than a fourfold reduction in the total liver and mitochondrial calcium accumulation following reflow. This apparent protective effect of chlorpromazine was not the result of a mere delay in the process of liver cell death, because there was a significant reduction of hepatocyte necrosis at 48 hr after a single initial dose of chlorpromazine. Pretreatment with chlorpromazine in a nonreperfused rat myocardial ischemia model prevented the appearance of ischemic cell death at 24 hr and inhibited calcium accumulation attendant with myocyte necrosis (*16*).

Accelerated degradation of phospholipids was reduced by 33% at 12 hr. Chlorpromazine also demonstrated in vitro preservation of postreperfusion myocardial ultrastructure and contractile function in the rabbit interventricular septum (*17*). In an isolated rabbit heart perfusion model, addition of chlorpromazine to the perfusate after a calcium-free period reduced the amount of protein and creatine kinase release (*22*) and prevented depression of the contractile function (*19*) caused by the calcium paradox. A recent study by Scott et al. (*21*) demonstrated that phenothiazines (and structurally dissimilar calmodulin inhibitors) were capable of preserving the sarcolemmal integrity of myocytes in culture by interfering with the calcium-dependent process that resulted in spontaneous attrition of these cells in culture. Antimyosin antibody binding (used as an indicator of the irreversible myocyte injury) (*41*) was diminished by the addition of phenothiazines proportional to their relative calmodulin inhibitory activity. Increasing calcium concentration in the presence of varying concentrations of phenothiazines demonstrated competitive inhibition of calcium-mediated membrane injury.

Antimyosin localization is inversely related to ^{201}Tl and ^{99m}Tc-sestamibi distributions in acute experimental myocardial infarction (*42,43*). It also has an inverse exponential relationship to radiolabeled microsphere-determined regional myocardial blood flow (*42*). Furthermore, the extent of infarction delineated by radiolabeled antimyosin is reported to be identical to that of triphenyl tetrazolium chloride staining in experimental (*13,28*) and clinical postmortem assessments (*44–46*). The specificity of antimyosin for the delineation of irreversibly necrotic myocardium hours to days after the initial insult was also well documented (*13–15,41*). Although antimyosin administered during coronary occlusion prior to reperfusion should be able to bind myosin in myocytes with small breaches in the sarcolemma, whether some of these

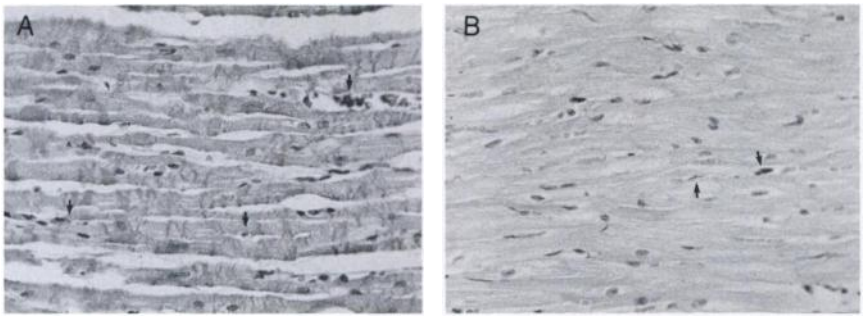

FIGURE 8. Using the ex vivo scans for both radiolabels, histologic sections of the region of the infarct common to both pre- and postreperfusion images and of the areas from the infarct border were examined. Myocytic necrosis with contraction bands is seen in the region of radioisotope discordance in a control animal (A). By contrast, no contraction bands are seen in the TFP-treated animal (B) (hematoxylin and eosin, ×100). Arrows indicate areas of monastral blue in the sections, confirming that both were from the myocardial zone at risk.

antimyosin-positive cells are amenable to intervention at the time of reperfusion is not known.

Cell membrane disruption is the hallmark of irreversible myocardial cell injury (*13–15*). However, it is possible that if membrane integrity is restored rapidly, before the intracellular contents are lost, cellular viability may be maintained. Microinjection techniques have been used successfully for delivery of reagents into cells (*47*). This process, by necessity, induces holes in the membrane, which are much larger than the holes that would permit the entry of macromolecules. Yet these manipulated cells with holes punched in the cell membrane subsequently seal them-

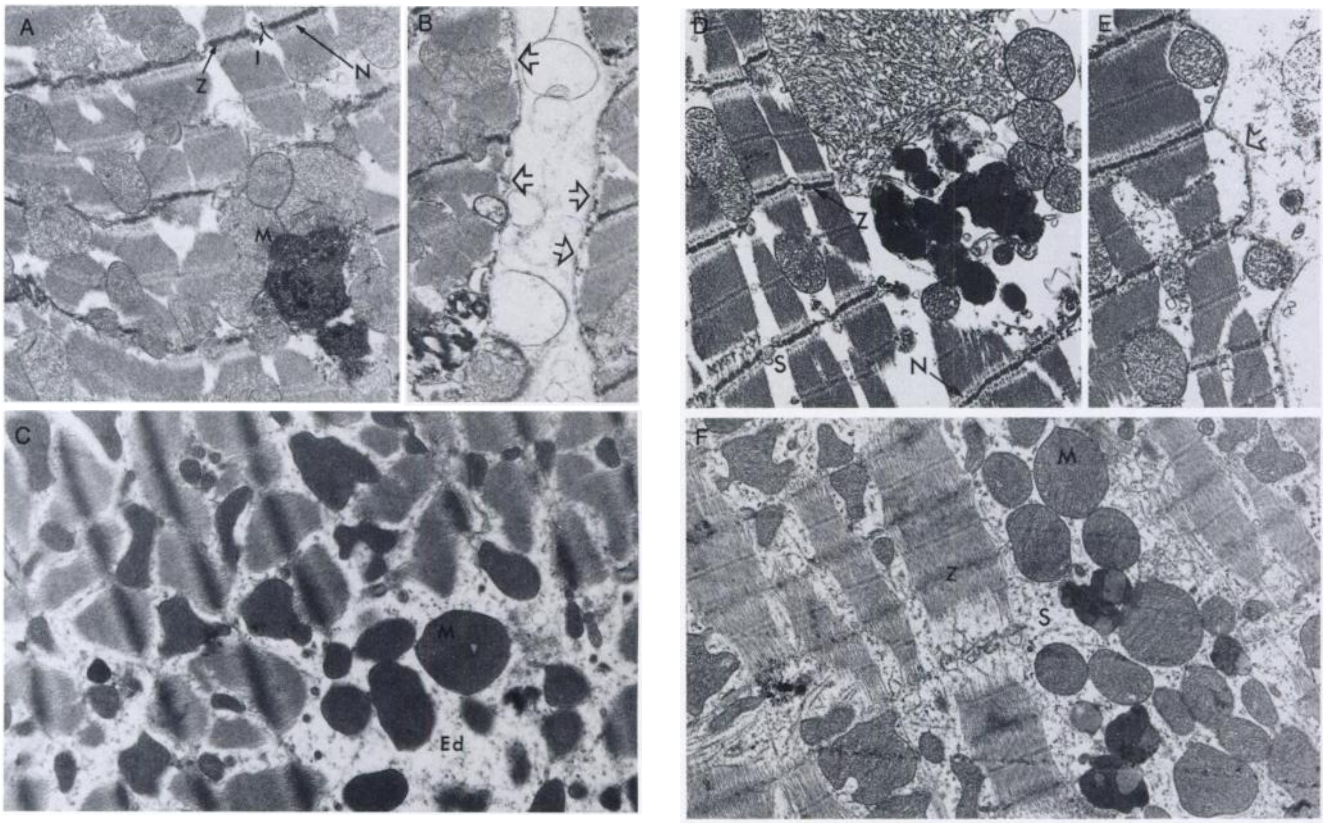

FIGURE 9. Transmission electron micrographs from the peripheral and central infarct zone from placebo- and TFP-treated animals. The infarct periphery (A and B) and the infarct center (D and E) in a representative control animal demonstrated irreversible ischemic injury. There was generalized swelling of the mitochondria (M), associated with amorphous electron-dense deposits or spicular aggregates in virtually every mitochondrial profile. The myofibrils were relaxed, the I bands (I) were prominent, and the N line (N) was observed on either side of the Z line (Z). Note the clarity of the sarcoplasmic space (S), suggesting a loss of glycogen granules. Sarcolemmal stretches demonstrated either prominent breaks or a loss of plasmalemma (arrows, B and E). The myocardium treated with TFP simultaneously with reperfusion demonstrated ultrastructural evidence of myocardial protection (C and F). Although the infarct center (F) showed evidence of degenerated mitochondria and relaxed myofibrils, glycogen granules were only partially lost. The infarct periphery (C) showed preservation of the mitochondria, absence of I bands and preservation of glycogen granules. Cellular edema (Ed) was inevitable. The uninvolved posterior left ventricular myocardium was ultrastructurally normal in both placebo- and TFP-treated animals. Chromatin of the nucleus was evenly distributed, plasmalemma and basal lamina were intact, glycogen granules were abundantly present and mitochondria appeared normal with tightly packed cristae (data not shown) (magnification ×12,000).

selves and remain viable. Fab fragments of antibodies are 35 × 65 Å (*48*) and should be able to traverse membrane disruption as small as 70 to 80 Å in diameter. The frankly necrotic myocytes in Figure 9E demonstrate sarcolemmal breaches of 1 to 3 cm, which are equivalent to a diameter of 0.3 to 0.83 μ. Therefore, breaches of only 0.03 mm (equivalent to a diameter of 80 Å) would be required to allow entry of Fab. It may be possible that during occlusion myocytes at risk develop sarcolemmal holes large enough to permit antibody access and, with the passage of time, progress to frank myocyte necrosis only. However, some of these small lesions should also be able to seal themselves with a return to favorable conditions, such as reperfusion and/or pharmaceutical intervention.

CONCLUSION

This study demonstrates the feasibility of dual-labeled radioisotope antimyosin for the assessment of myocardial infarct size at two different time points. Although there might be no direct clinical applicability of this method, it might provide an experimental tool for the evaluation of the pharmaceutical interventions. The study also suggests the potential benefit of acute salvage of critically injured myocytes. The long-term efficacy of membrane stabilization, however, requires further study.

ACKNOWLEDGMENT

Funding for this study was provided by departmental and discretionary funds and did not involve industrial support.

REFERENCES

1. Braunwald E, Kloner RA. Myocardial reperfusion: a double edged sword? *J Clin Invest* 1985;76:1713–1719.
2. Flaherty JT, Weisfeldt ML. Reperfusion injury. *Free Radic Biol Med* 1988; 5:409–419.
3. Simpson PJ, Lucchesi BR. Free radicals and myocardial ischemia and reperfusion injury. *J Lab Clin Med* 1987;110:13–30.
4. Kloner RA, Przyklenk K, Whittaker P. Deleterious effects of oxygen radicals in ischemia/reperfusion. *Circulation* 1989;80:1115–1127.
5. Cohen MV. Free radicals in ischemic reperfusion myocardial injury: is this the time for clinical trials? *Ann Intern Med* 1989;111:918–931.
6. Reimer KA, Jennings RB, Cobb FR, et al. Animal models for protecting ischemic myocardium (AMPIM): results of the NHLBI cooperative study. Comparison on unconscious and conscious dog models. *Circ Res* 1985;56: 651–665.
7. Jolly SR, Kane WJ, Bailei MB, Abrams GD, Lucchesi BR. Canine myocardial reperfusion injury: its reduction by the combined administration of superoxide dismutase and catalase. *Circ Res* 1984;54:277–285.
8. Ambrosio G, Becker LC, Hutchins GM, Weisman HF, Weisfeldt ML. Reduction in experimental infarct size by recombinant human superoxide dismutase: insights into the pathophysiology of reperfusion injury. *Circulation* 1986;74:1424–1433.
9. Uraizee A, Reimer KA, Murray CE, Jennings RB. Failure of superoxide dismutase to limit size of myocardial infarction after 40 minutes of ischemia and 4 days of reperfusion in dogs. *Circulation* 1987;75:473–480.
10. Przyklenk K, Kloner RA. "Reperfusion injury" by oxygen-derived free radicals? Effect of superoxide dismutase plus catalase, given at the time of reperfusion, on myocardial infarct size, contractile function, coronary microvasculature, and regional myocardial blood flow. *Circ Res* 1989;64:86–96.
11. Babbitt DG, Virmani R, Forman MB. Intracoronary adenosine administered after reperfusion limits vascular injury after prolonged ischemia in the canine model. *Circulation* 1989;80:1388–1399.
12. Farb A, Kolodgie FD, Jenkins M, Virmani R. Myocardial infarct extension during coronary artery occlusion: pathologic evidence. *J Am Coll Cardiol* 1993;21:1245–1253.
13. Khaw BA, Fallon JT, Strauss HW, Haber E. Myocardial infarct imaging of antibodies to canine cardiac myosin with indium-111-DTPA. *Science* 1980; 209:295–297.
14. Khaw BA, Beller GA, Haber E, Smith TW. Localization of cardiac myosin-specific antibody in myocardial infarction. *J Clin Invest* 1976;58:439–446.
15. Khaw BA, Fallon JT, Beller GA, Haber E. Specificity of localization of myosin-specific antibody fragments in experimental myocardial infarction: histologic, histochemical, autoradiographic and scintigraphic studies. *Circulation* 1979;60:1527–1531.
16. Chien KR, Pfau RG, Farber JL. Ischemic myocardial cell injury. Prevention by chlorpromazine of an accelerated phospholipid degeneration and associated membrane dysfunction. *Am J Pathol* 1979;97:505–530.
17. Burton KP, Hagler HK, Willerson JT, Buja LM. Abnormal lanthanum accumulation due to ischemia in isolated myocardium: effect of chlorpromazine. *Am J Physiol* 1981;241:H714–H723.
18. Nunnally RL, Bottomly PA. Assessment of pharmacological treatment of myocardial infarction by phosphorus-31 NMR with surface coils. *Science* 1981;211:177–180.
19. Rabkin SW. Effect of chlorpromazine on myocardial damage in the calcium paradox. *J Cardiovasc Pharmacol* 1987;9:486–492.
20. Slezak J, Tribulova N, Gabauer I, et al. Diminution of injury in reperfused ischemic myocardium by phenothiazines. A quantitative morphological study. *Biomed Biochim Acta* 1987;46:S606–S609.
21. Scott JA, Khaw BA, Fallon JT, et al. The effect of phenothiazines upon maintenance of membrane integrity in the cultured myocardial cell. *J Mol Cell Cardiol* 1986;18:1243–1254.
22. Schaffer SW, Burton KP, Jones HP, Oei HH. Phenothiazine protection in calcium overload-induced heart failure: possible role for calmodulin. *Am J Physiol* 1983;244:H32–H34.
23. Okumura K, Ogawa K, Satake T. Effects of trifluoperazine and chlorpromazine on calcium-repleted injury in isolated ventricular strips. *Basic Res Cardiol* 1985;80:556–563.
24. Prozialeck WC, Weiss B. Inhibition of calmodulin by phenothiazines and related drugs: structure-activity relationships. *J Pharmacol Exp Ther* 1982; 222:509–518.
25. Khaw BA, Mattis JA, Melincoff G, et al. Monoclonal antibody to cardiac myosin: imaging of experimental myocardial infarction. *Hybridoma* 1984;3: 11–23.
26. Hnatowich DL, Layne WW, Childs RL, et al. Radioactive labeling of antibody: a simple and efficient method. *Science* 1983;220:613–615.
27. Hunter WM, Greenwood FC. Preparation of I-131 labeled human growth harmone of high specific activity. *Nature* 1962;194:495–496.
28. Khaw BA, Strauss HW, Moore R, et al. Myocardial damage delineated by indium-111 antimyosin Fab and technetium-99m pyrophosphate. *J Nucl Med* 1987;28:76–82.
29. Ostrzega E, Maddahi J, Honma H, et al. Quantification of left ventricular myocardial mass in humans by nuclear magnetic resonance imaging. *Am Heart J* 1989;117:444–452.
30. Khaw BA, Klibanov A, O'Donnell SM, et al. Gamma imaging with negative charge-modified monoclonal antibody: modification with synthetic polymers. *J Nucl Med* 1991;32:1742–1751.
31. Dixon WJ, Brown MB, Engelman L, Hill MA, Jennrich RI. *BMDP statistical software manual*, vol. 2. Berkeley, CA: University of California Press; 1988:1045.
32. Morrison DF. *Multivariate statistical methods*. New York: McGraw-Hill; 1976:33–34.
33. Seeman P. Membrane actions of anesthetics and tranquilizers. *Pharmacol Rev* 1972;24:583–656.
34. Guth PS, Spirites MA. The phenothiazine tranquilizer: biochemical and biophysical actions. *Int Rev Neurobiol* 1964;7:231–278.
35. Dhalla NS, Lee SL, Torkess S, Canageo V, Bharya V. Effect of chlorpromazine and imipramine on rat heart subcellular membranes. *Biochem Pharmacol* 1980;29:629–633.
36. Cheung WY. Calmodulin plays a pivotal role in cellular replication. *Science* 1980;207:19–27.
37. Farber JL, El-Mofty SK. The biochemical pathology of liver cell necrosis. *Am J Pathol* 1975;81:237–250.
38. Irvine RF, Hemington N, Dawson RMC. The hydrolysis of phosphatidylinositol by lysosomal enzymes of rat liver and brain. *Biochem J* 1978;176: 475–484.
39. Beckman JK, Owens K, Knauer TE, Weglicki WB. Hydrolysis of sarcolemma by lysosomal lipases and inhibition by chlorpromazine. *Am J Physiol* 1982;242:H652–H656.

40. Chein KR, Abrams J, Pfau RG, Farber JL. Prevention by chlorpromazine of ischemic liver cell death. *Am J Pathol* 1977;88:539–558.
41. Khaw BA, Scott J, Fallon JT, Haber E. Myocardial injury quantitation by cell sorting method with antimyosin fluorescence spheres. *Science* 1982; 217:1050–1053.
42. Khaw BA, Strauss HW, Pohost GM, et al. Relation of immediate and delayed thallium-201 distribution to localization of iodine-125 antimyosin antibody in acute experimental myocardial infarction. *Am J Cardiol* 1983; 51:1428–1432.
43. Khaw BA, Mousa SA. Comparative assessment of experimental myocardial infarction with 99mTc-hexakis-t-butyl-isonitrile (sestamibi), ^{111}In-antimyosin and ^{201}Tl. *Nucl Med Commun* 1991;12:853–863.
44. Jain D, Lahiri A, Crawley JCW, Raftery EB. Indium-111 antimyosin imaging in a patient with acute myocardial infarction: postmortem correlation between histopathologic and autoradiographic extent of myocardial necrosis. *Am J Cardiac Imaging* 1988;2:158–161.
45. Jain D, Crawley JC, Lahiri A, Raftery EB. Indium-111-antimyosin images compared with TTC staining in a patient six days after myocardial infarction. *J Nucl Med* 1990;31:231–233.
46. Hendel RC, McSherry BA, Leppo JA. Myocardial uptake of indium-111-labeled antimyosin in acute subendocardial infarction: clinical, histochemical and autoradiographic correlation of myocardial necrosis. *J Nucl Med* 1990;31:1851–1853.
47. Graessmann A. Mikrochirurgishe Zellkern transplantation bei saugetierzellen. *Exp Cell Res* 1970;60:373–380.
48. Green NM. Electron microscopy of immunoglobulins. *Adv Immunol* 1969; 11:1–30.